Particle-number fluctuation of pairing correlations for Dy isotopes *

CHENG Ming-Jian(程明建) LIU Lang(刘朗)[1)] ZHANG Yi-Xin(张逸新)

School of Science, Jiangnan University, Wuxi 214122, China

Abstract: Within the relativistic mean field (RMF) theory, the ground state properties of dysprosium isotopes are studied using the shell-model-like approach (SLAP), in which pairing correlations are treated with particle-number conservation, and the Pauli blocking effects are taken into account exactly. For comparison, calculations of the Bardeen–Cooper–Schrieffer (BCS) model with the RMF are also performed. It is found that the RMF+SLAP calculation results, as well as the RMF+BCS ones, reproduce the experimental binding energies and one- and two-neutron separation energies quite well. However, the RMF+BCS calculations give larger pairing energies than those obtained by the RMF+SLAP calculations, in particular for nuclei near the proton and neutron drip lines. This deviation is discussed in terms of the BCS particle-number fluctuation, which leads to the sizable deviation of pairing energies between the RMF+BCS and RMF+SLAP models, where the fluctuation of the particle number is eliminated automatically.

Key words: relativistic mean field theory, shell-model-like approach, pairing correlations, particle-number fluctuation

PACS: 21.60.Jz, 21.60.Cs **DOI:** 10.1088/1674-1137/39/10/104102

1 Introduction

Relativistic mean field (RMF) theory [1], as a microscopic model in nuclear physics, has been widely used. It has been proven that RMF theory can describe lots of nuclear phenomena successfully [2–7], including stable nuclei [2, 4] and exotic nuclei [5, 8]. It offers good descriptions for many nuclear properties, for example, magnetic moments [9], antimagnetic rotation [10], single-particle resonant states [11], collective excitation states [12], superdeformation in the superheavy nuclei [13], giant resonances and identical bands in rotating superdeformed nuclei [14] and gives more naturally the spin-orbit potential and the origin of the pseudospin symmetry [15, 16] as a relativistic symmetry [17–20].

In order to investigate nuclear properties of the open shell nuclei, RMF theory should be added with the suitable treatment of the pairing correlations, which play an essential role in the properties of nuclei. So far, the most commonly used methods, the Bardeen–Cooper–Schrieffer (BCS) approximation and Bogoliubov transformation, have become standard in nuclear physics literature [4, 21]. Recently, a separable form of pairing interaction has been introduced and successfully applied in the description of both static and dynamic properties of superfluid nuclei [22]. Moreover, the shell-model-like approach (SLAP) [23] has shown several advantages over the conventional methods—BCS approximation and Bogoliubov transformation. SLAP can overcome their difficulties, including the violation of particle number conservation, unreasonable treatment of the Pauli blocking effects and spurious states [24]. Since the Pauli blocking effects are strictly taken into account by diagonalizing the pairing Hamiltonian in the multiparticle configuration (MPC) space directly, both even–even and odd-A nuclei can be treated in the same framework in the SLAP. SLAP has been applied successfully for investigating odd–even differences in moments of inertia (MOIs) [25], nonadditivity in MOIs [26], identical bands [27], nuclear pairing reduction under rotation [28], high-spin states and high-K isomers in the rare-earth, the actinide region and superheavy nuclei [29, 30], α-cluster structures of light nuclei [31] and nuclear antimagnetic rotation [32].

As one of the quantum fluctuations, the particle-number uncertainty in the BCS approximation or Bogoliubov transformation and its effect in nuclei are worth evaluating and comparing with the benchmark of the particle number conserving SLAP. In this work, SLAP and BCS are applied to study the ground state proper-

Received 21 November 2014

∗ Supported by Fundamental Research Funds for the Central Universities (JUSRP1035), National Natural Science Foundation of China (11305077)

1) E-mail: liulang@jiangnan.edu.cn

ties of Dy isotopes in the RMF theory. A brief formalism is presented in Section 2. In Section 3, we give the numerical details, results and discussion for Dy isotopes. Finally, a brief conclusion is given in Section 4.

2 Theoretical framework

The starting point of the RMF theory is the effective Lagrangian, written as:

$$\begin{aligned}\mathcal{L} = {} & \bar{\psi}(\mathrm{i}\gamma^\mu\partial_\mu - M)\psi + \frac{1}{2}\partial^\mu\sigma\partial_\mu\sigma - \frac{1}{2}m_\sigma^2\sigma^2 \\ & - \frac{1}{3}g_2\sigma^3 - \frac{1}{4}g_3\sigma^4 - g_\sigma\bar{\psi}\sigma\psi - \frac{1}{4}\Omega^{\mu\nu}\Omega_{\mu\nu} \\ & + \frac{1}{2}m_\omega^2\omega^\mu\omega_\mu - g_\omega\bar{\psi}\gamma^\mu\psi\omega_\mu + \frac{1}{4}g_4(\omega^\mu\omega_\mu)^2 \\ & - \frac{1}{4}R^{\mu\nu}\cdot R_{\mu\nu} + \frac{1}{2}m^2{}_\rho\rho^\mu\cdot\rho_\mu - g_\rho\bar{\psi}\gamma^\mu\tau\cdot\psi\rho_\mu \\ & - \frac{1}{4}F^{\mu\nu}F_{\mu\nu} - e\bar{\psi}\gamma^\mu\frac{1-\tau_3}{2}A_\mu\psi, \end{aligned} \tag{1}$$

where the field tensors of the vector mesons and the electromagnetic field take the forms:

$$\begin{cases} \Omega^{\mu\nu} = \partial^\mu\omega^\nu - \partial^\nu\omega^\mu \\ R^{\mu\nu} = \partial^\mu\rho^\nu - \partial^\nu\rho^\mu - 2g_\rho\rho^\mu\times\rho^\nu \\ F^{\mu\nu} = \partial^\mu A^\nu - \partial^\nu A^\mu. \end{cases} \tag{2}$$

With this Lagrangian of the RMF theory, the effective nucleon–nucleon interaction can be described by the exchange of three mesons [3–5]: the scalar meson δ mediates the medium-range attraction between the nucleons; the vector meson ω^μ mediates the short-range repulsion; and the isovector–vector meson ρ^μ provides the isospin dependence of the nuclear force.

The Dirac equation, which describes the nucleon motion, reads:

$$\{-\mathrm{i}\alpha\cdot\nabla + V(\boldsymbol{r}) + \beta[M + S(\boldsymbol{r})]\}\psi_i = \epsilon_i\psi_i, \tag{3}$$

where the vector and scale potentials are defined as

$$\begin{cases} V_\mu(\boldsymbol{r}) = g_\omega\omega_\mu(\boldsymbol{r}) + g_\rho\tau\cdot\rho_\mu(\boldsymbol{r}) + e\frac{1-\tau_3}{2}A_\mu(\boldsymbol{r}) \\ S(\boldsymbol{r}) = g_\sigma\sigma(\boldsymbol{r}). \end{cases} \tag{4}$$

For describing the mesons, the Klein–Gordon equations can be written as:

$$\begin{cases} [-\Delta + m_\sigma^2]\sigma(\boldsymbol{r}) = -g_\sigma\rho_{\mathrm{s}}(\boldsymbol{r}) - g_2\sigma^2(\boldsymbol{r}) - g_3\sigma^3(\boldsymbol{r}) \\ [-\Delta + m_\omega^2]\omega^\mu(\boldsymbol{r}) = g_\omega j^\mu(\boldsymbol{r}) - g_4(\omega^\nu\omega_\nu)\omega^\mu(\boldsymbol{r}) \\ \left[-\Delta + m_\rho^2\right]\rho^\mu(\boldsymbol{r}) = g_\rho j^\mu(\boldsymbol{r}) \\ -\Delta A^\mu(\boldsymbol{r}) = e j_\rho^\mu(\boldsymbol{r}), \end{cases} \tag{5}$$

where the source terms and densities for the mesons and the photons are:

$$\begin{cases} \rho_{\mathrm{s}}(\boldsymbol{r}) = \sum_{i=1}^{A}\bar{\psi}_i\psi_i \\ j^\mu(\boldsymbol{r}) = \sum_{i=1}^{A}\bar{\psi}_i\gamma^\mu\psi_i \\ j^\mu(\boldsymbol{r}) = \sum_{i=1}^{A}\bar{\psi}_i\gamma^\mu\tau\psi_i \\ j_{\mathrm{p}}^\mu(\boldsymbol{r}) = \sum_{i=1}^{A}\bar{\psi}_i\gamma^\mu\frac{1-\tau_3}{2}\psi_i. \end{cases} \tag{6}$$

Usually, the meson field operators in Eq. (5) are replaced by their corresponding expectation values. In such a way, the coupled equations can be solved by self-consistent iteration. In the system considered in this work, there are no nuclear currents and the spatial components of ω, ρ , and A disappear. As the time reversal symmetry is well conserved, only the time-like parts ω^0, ρ^0, and A^0 are left. Charge conservation guarantees that only the 3-component of the isovector ρ survives. For axially deformed nuclei, it is useful to work with cylindrical coordinates: $x = r_\perp\cos\varphi$, $y = r_\perp\sin\varphi$ and z. The Dirac wave function ψ_i for the nucleon with the index i is labeled by the quantum numbers Ω_i, π_i and t_i , where $\Omega_i = m_{\ell i} + m_{si}$ is the eigenvalue of the angular momentum operator J_z, π_i is the parity, and t_i is the isospin.

The Dirac spinor ψ_i has the form:

$$\psi_i = \begin{pmatrix} f_i(\boldsymbol{r}) \\ \mathrm{i}g_i(\boldsymbol{r}) \end{pmatrix} = \frac{1}{2\pi}\begin{pmatrix} f_i^+(z, r_\perp)\mathrm{e}^{\mathrm{i}\left(\Omega_i - \frac{1}{2}\right)\varphi} \\ f_i^-(z, r_\perp)\mathrm{e}^{\mathrm{i}\left(\Omega_i + \frac{1}{2}\right)\varphi} \\ \mathrm{i}g_i^+(z, r_\perp)\mathrm{e}^{\mathrm{i}\left(\Omega_i - \frac{1}{2}\right)\varphi} \\ \mathrm{i}g_i^-(z, r_\perp)\mathrm{e}^{\mathrm{i}\left(\Omega_i + \frac{1}{2}\right)\varphi} \end{pmatrix}\chi_{t_i}(t). \tag{7}$$

For each solution with positive ψ_i, Ω_i, there is a time-reversed solution with the same energy $\psi_{\bar{i}} = -\mathrm{i}\sigma_\nu K\psi_i$. Therefore, the densities can be represented as:

$$\rho_{\mathrm{s,v}} = 2\sum_{i>0}n_i[(|f_i{}^+|^2 + |f_i{}^-|^2) \mp (|g_i{}^+|^2 + |g_i{}^-|^2)]. \tag{8}$$

We can obtain ρ_3 and ρ_{c} in a similar way. These densities serve as the sources for the fields σ, ω^0, ρ^0 and A^0. The occupation probabilities n_i can be obtained in SLAP with the the pairing correlation considered.

The total energy of the system is:

$$E_{\mathrm{RMF}} = E_{\mathrm{nucleon}} + E_\sigma + E_\omega + E_\rho + E_{\mathrm{c}} + E_{\mathrm{CM}} + E_{\mathrm{pair}}, \tag{9}$$

with

$$\begin{cases} E_{\rm nucleon}=\sum\limits_i \epsilon_i \\ E_\sigma=-\dfrac{1}{2}\int {\rm d}^3r \left\{ \begin{array}{l} g_\sigma \rho_{\rm s}(\boldsymbol{r})\sigma(r)+\left[\dfrac{1}{3}g_2\sigma(\boldsymbol{r})^3 \right. \\ \left. +\dfrac{1}{2}g_3\sigma(\boldsymbol{r})^4\right] \end{array} \right\} \\ E_\omega=-\dfrac{1}{2}\int {\rm d}^3r\{g_\omega\rho_{\rm v}(\boldsymbol{r})\omega^0(\boldsymbol{r})-\dfrac{1}{2}g_4\omega^0(\boldsymbol{r})^4\} \\ E_\rho=-\dfrac{1}{2}\int {\rm d}^3r g_\rho\rho_3(\boldsymbol{r})\rho^{00}(\boldsymbol{r}) \\ E_{\rm c}=-\dfrac{{\rm e}^2}{8\pi}\int {\rm d}^3r\rho_{\rm c}(r)A^0(\boldsymbol{r}) \\ E_{\rm CM}=-\dfrac{3}{4}41A^{-1/3} \\ E_{\rm pair}=\langle\psi^\beta|H_{\rm pair}|\psi^\beta\rangle, \end{cases} \tag{10}$$

where $E_{\rm nucleon}$ is the summation of the energies of nucleon ϵ_i; E_σ, E_ω, E_ρ and $E_{\rm c}$ are the energies of the meson fields and the Coulomb fields, $E_{\rm CM}$ is the correction for the center-of-mass motion, and $E_{\rm pair}$ is the pairing energy.

The main idea of SLAP in dealing with the pairing correlations is diagonalizing the pairing Hamiltonian in the MPC space directly. Using the single-particle levels calculated from the RMF theory, the SLAP can be chosen to treat the nuclear pairing correlations.

The Hamiltonian is given by:

$$H=H_{\rm s.p.}+H_{\rm pair}=\sum_i \epsilon_i a_i^\dagger a_i - G\sum_{i,j>0}^{j\neq i} a_i^\dagger a_{\bar{i}}^\dagger a_{\bar{j}} a_j. \tag{11}$$

For an even ($N=2n$) particle system, the MPCs are constructed as follows:

(a) The fully paired configuration (seniority s=0):

$$|c_1\bar{c_1}\cdots c_n\bar{c_n}\rangle = a_{c_1}^\dagger a_{\bar{c_1}}^\dagger\cdots a_{c_n}^\dagger a_{\bar{c_n}}^\dagger|0\rangle. \tag{12}$$

(b) The configuration with two unpaired particles (seniority s=2):

$$|i\bar{j}c_1\bar{c}_1\cdots c_{n-1}\bar{c}_{n-1}\rangle = a_i^\dagger a_{\bar{j}}^\dagger a_{c_1}^\dagger a_{\bar{c}_1}^\dagger\cdots a_{c_{n-1}}^\dagger a_{\bar{c}_{n-1}}^\dagger|0\rangle, \tag{13}$$

and so on.

The others can be constructed similarly [19, 20].

For the axially deformed nuclei, the MPC space can be written as:

$$\begin{aligned} {\rm MPC\ \ space} = & (s=0,K=0^+)\oplus(s=2,K=0^+) \\ & \oplus\ (s=2,K=1^+)\oplus(s=2,K=2^+) \\ & \oplus\ (s=4,K=0^+)\oplus(s=4,K=1^+) \\ & \oplus\ (s=4,K=2^+)\oplus\cdots\oplus\cdots. \end{aligned} \tag{14}$$

For the ground states and the low-lying excited states of nuclei, the number of major MPCs is limited. Only the configuration with lower energy multiparticles contributes significantly. An energy cutoff $E_{\rm c}$ is introduced to diagonalize the Hamiltonian H in Eq. (11). E_i is the energy of the ith configuration. If $E_i-E_0\leqslant E_{\rm c}$, the corresponding wave function will be written as:

$$\begin{aligned} \psi^\beta = & \sum_{c_1\cdots\rho_n} v^\beta_{c_1\cdots c_n}|c_1\bar{c}_1\cdots c_n\bar{c}_n\rangle \\ & +\sum_{i,j}\sum_{c_1\cdots c_{n-1}} v^{\beta(ij)}_{c_1\cdots c_{n-1}}|i\bar{j}c_1\bar{c}_1\cdots c_{n-1}\bar{c}_{n-1}\rangle, \end{aligned}$$

where $\beta=0$ (ground state), 1, 2, 3, $\cdots$ (excited states). The occupation probability of the ith level for state β is:

$$\begin{aligned} n_i^\beta = & \sum_{c_1\cdots c_{n-1}} |V^\beta_{c_1\cdots c_{n-1},i}|^2+\sum_{i,j}\sum_{c_1\cdots c_{n-2}} |V^{\beta(i,j)}_{c_1\cdots c_{n-2},i}|^2 \\ & +\cdots,\ i=1,2,3,\cdots. \end{aligned} \tag{15}$$

Replacing the occupation number n_i in Eq. (8) by n_i^β, the source terms in Eq. (5) are obtained, which generate new meson fields and a new electromagnetic field. These new fields then are adopted to calculate the vector and scalar potentials in Eq. (4). Using these new potentials, the Dirac equation [Eq. (3)] is solved again. These procedures should be repeated until the results converge to the given precision. More details of RMF+SLAP can be found in Ref. [23].

3 Results and discussion

In this work, we select the effective interaction PK1 [33] to solve the Dirac equations and the Klein–Gordon equations. The Dirac equations of the nucleons and the Klein–Gordon equations of the mesons and photons are solved by expansion in the harmonic oscillator basis with 18 oscillator shells for both the fermions and the bosons. The deformation of harmonic oscillator basis β_0 should be reasonably set to obtain the lowest energy. For Dy isotopes, β_0 is set to 0.2. The pairing strengths $G_{\rm n}$ (neutron), $G_{\rm p}$ (proton) and truncation energy $E_{\rm c}$ are the three most important parameters in SLAP. With the truncated energy fixed, the pairing strengths are adopted by reproducing the experimental odd–even mass differences. The odd–even mass differences are defined as:

$$\Delta_n=\frac{1}{2}[B(N-1,Z)+B(N+1,Z)]-B(N,Z). \tag{16}$$

In the following calculations for the Dy isotopes, the truncation energy is reasonably fixed to 15 MeV, and the pairing strengths $G_{\rm n}$ for neutrons and $G_{\rm p}$ for protons are set to $45/A$ MeV and $54/A$ MeV respectively in the RMF+SLAP calculations. In the RMF+BCS calculations the pairing strength $G_{\rm n}$ is set to $19.5/A$ MeV, and $G_{\rm p}$ is set to $31/A$ MeV.

Figure 1 demonstrates the odd–even mass differences of Dy isotopes calculated by RMF+SLAP and RMF+BCS with PK1 in comparison with experimental

data [34] as a function of neutron number N. It is observed that both the RMF+BCS and RMF+SLAP calculations reliably reproduce the experimental odd–even mass differences with the chosen pairing strengths and the corresponding configuration cut-off energy.

One- and two-neutron separation energies are sensitive quantities to test a microscopic theory. Fig. 2 depicts the binding energies per nucleon E/A and one- and two-neutron separation energies S_n and S_{2n}, for Dy isotopes calculated by RMF+SLAP and RMF+BCS with PK1 as a function of neutron number N in comparison with the experimental data [34]. We can see that the binding energies per nucleon and one- and two-neutron separation energies can be well described in both calculations of RMF+SLAP and RMF+BCS.

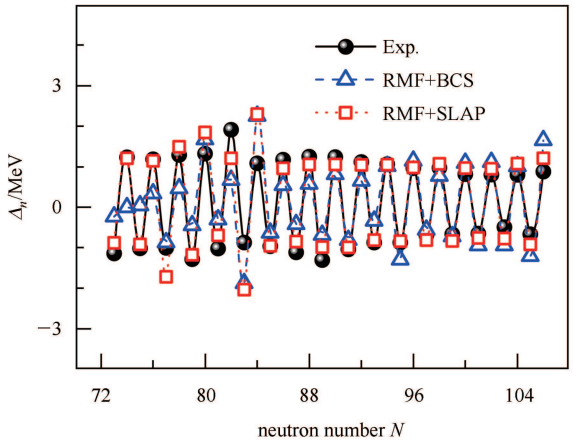

Fig. 1. (color online) Odd–even mass differences of Dy isotopes calculated by RMF+SLAP (open squares) and RMF+BCS (open triangles) in comparison with experimental data [30] (full circles).

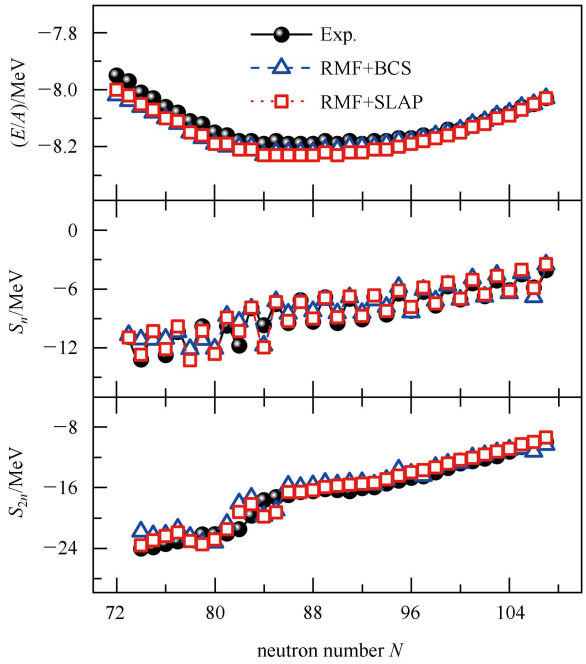

Fig. 2. (color online) Binding energies per nucleon E/A (top panel), one- (middle panel) and two-neutron separation energies (bottom panel) calculated by RMF+SLAP (open squares) and RMF+BCS (open triangles) in comparison with experimental data [34] (full circles).

In Fig. 3, we present the neutron, proton and total pairing energies for Dy isotopes calculated by RMF+SLAP and RMF+BCS with PK1 as a function of neutron number N. It is shown that both the RMF+BCS and RMF+SLAP calculation results for neutron pairing energies are small when the neutron number N is around 82. However, with increasing neutron number, the differences of neutron pairing energies between these two calculation results is obviously increased. In the case of the proton, however, the calculation results of RMF+BCS and RMF+SLAP have large deviations when the neutron number N is small (about $\leqslant 92$). The differences between these two calculations diminish rapidly with the increasing of neutron number and provide almost the same pairing energies when the neutron number N is over 95. For the total pairing energies, it is observed that the RMF+BCS calculations always give larger pairing energies than those of the RMF+SLAP calculations, in particular for nuclei near the proton and neutron drip lines. Moreover, it can be seen that the odd–even staggering of the neutron pairing energies are

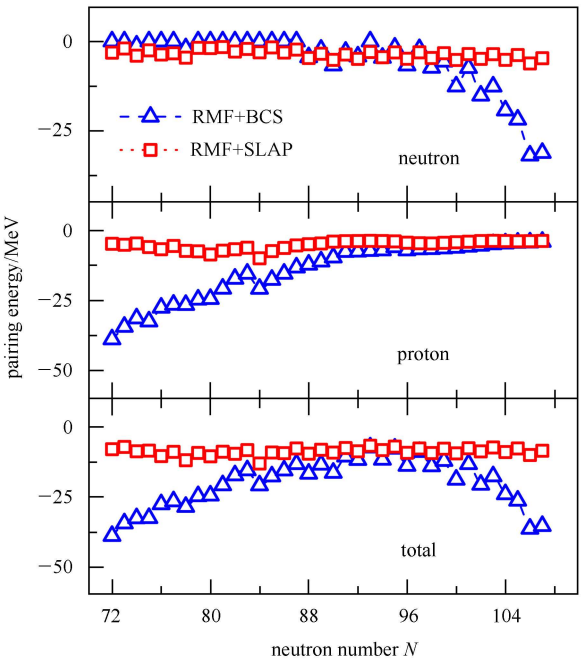

Fig. 3. (color online) Pairing energies of neutron (top panel), proton (middle panel), and the total (bottom panel) for Dy isotopes calculated by RMF+SLAP (open squares) and RMF+BCS (open triangles).

clearly revealed, due to the correct treatment of the Pauli blocking effects in SLAP. With the same fitting procedure for odd–even mass differences of the isotopes, although calculations of both RMF+BCS and RMF+SLAP can give reliable descriptions of the binding energies per nucleon E/A and one- and two-neutron separation energies S_n and S_{2n}, the RMF+BCS calculations overestimate the effect of pairing correlations of the ground states, in particular for nuclei near the proton and neutron drip lines.

In order to understand the behaviors of the pairing energies of the Dy isotopes in Fig. 3, we calculate the particle-number uncertainties of neutron and proton for Dy isotopes by RMF+BCS with PK1.

We define the particle-number uncertainty as $\dfrac{\Delta C(\tau)}{C(\tau)}$, where $C(\tau)$ is the expectation value of the particle-number, $\tau=\nu$ for neutron, $\tau=\pi$ for proton.

$\Delta C(\tau)$ is

$$(\Delta C(\tau))^2:=\langle BCS|\hat{C(\tau)}^2|BCS\rangle-C(\tau)^2=4\sum_{k>0}u_k^2v_k^2, \tag{17}$$

where v_k^2 represents the occupation probabilities and $u_k^2=1-v_k^2$ [35].

Figure 4 illustrates the particle-number uncertainties of neutron and proton for Dy isotopes calculated by RMF+BCS with PK1 as a function of neutron number N. It can be seen that the particle-number uncertainty of neutrons increases with the increasing of neutron number, and that of protons has the opposite tendency. In addition, the particle-number uncertainties for both neutrons and protons are between 1.5%–6%. The uncertainty of protons is always larger than that of neutrons. Compared with Fig. 3, it can be observed that the particle-number uncertainty of neutrons has a large value when sizable deviations of neutron pairing energies between the RMF+SLAP and RMF+BCS arise. Generally speaking, the particle-number uncertainty reduces with the increase of the particle number. Hence, in solid state physics, where $C\approx10^{23}$, the violation of particle number has no influence on any physical quantity. In nuclei, however, the violation of the invariance corresponding to the particle number in many cases gives rise to serious errors. One consequence has been presented in Fig. 3, where the BCS model overestimates the contribution of the pairing correlation. Moreover, the exotic phenomenon that the particle-number uncertainty of neutrons rises with the increase of neutron number can be understood by the fact that nuclei are not suitable to be investigated using the BCS model, due to their novel characteristics in comparison with stable nuclei. In addition, it is shown that the particle-number uncertainty of the neutron is zero when the neutron number N is around the magic number 82, whereas the BCS equation only gives an unphysical solution. This defect can be eliminated automatically in the RMF+SLAP model. This advantage will even be obvious when dealing with the excited states, e.g. rotational nuclei or hot nuclei.

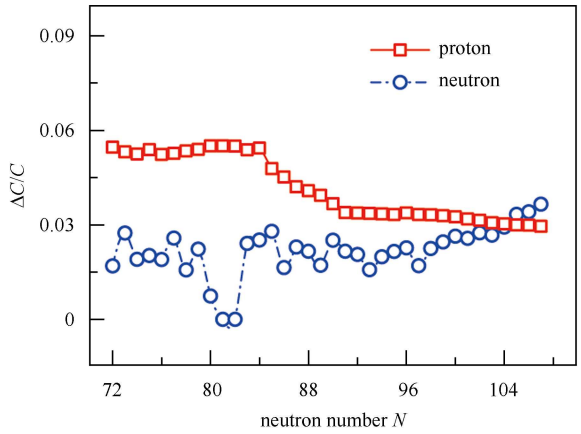

Fig. 4. (color online) Particle-number uncertainties of neutron (open circles) and proton (open squares) for Dy isotopes calculated by RMF+BCS.

4 Summary

RMF+SLAP calculations with the PK1 effective interaction have been used to study the ground state properties of Dy isotopes with the pairing correlations treated by a particle-number conserving method, which can treat the Pauli blocking effects exactly. Both the RMF+BCS and RMF+SLAP calculations reliably reproduce the experimental odd–even mass differences with the chosen pairing strengths and the corresponding configuration cut-off energy. The calculated ground state properties, including the binding energies and one- and two-neutron separation energies from both the RMF+BCS and RMF+SLAP models, agree well with the experimental data. The odd–even staggering is well reproduced, as shown in the binding energies, per-nucleon and one-neutron separation energies. Compared with the SLAP calculations, the BCS calculations always overestimate the effect of pairing correlations of the ground states, in particular for nuclei near the proton and neutron drip lines. This deviation is discussed in terms of the particle-number uncertainties in BCS method. The larger particle-number uncertainties lead to the sizable deviations of pairing energies between the RMF+SLAP and RMF+BCS models. The fluctuation of the particle number can be eliminated automatically in the RMF+SLAP model. In future, it should be interesting to investigate the effect of the particle-number fluctuation in nuclei excited states, e.g. rotational nuclei or hot nuclei.

References

1 Walecka J D. Ann. Phys., 1974, **83**(2): 491–529
2 Serot B D, Walecka J D. Adv. Nucl. Phys., 1986, **16**: 1
3 Reinhard P G. Rep. Prog. Phys., 1989, **52**: 439–514
4 Gambhir Y K, Ring P, Thimet A. Ann. Phys. New York, 1990, **194**: 132–179
5 Ring P. Prog. Part. Nucl. Phys., 1996, **37**: 193–263
6 MENG J, Toki H, ZHOU S G et al. Prog. Part. Nucl. Phys., 2006, **57**: 470–563
7 Vretenar D, Afanasiev A V, Lalazissis G A. Phys. Rep., 2005, **409**: 101–259
8 MENG J. Nucl. Phys. A, 1998, **635**: 3–42
9 ZHAO P W, PENG J, LIANG H Z et al. Phys. Rev. Lett., 2011, **107**: 122501
10 ZHAO P W, PENG J, LIANG H Z et al. Phys. Rev. C, 2012, **85**: 054310
11 CAO L G, MA Z Y. Phys. Rev. C, 2002, **66**: 024311
12 MA Z Y, Wandelt A, Giai N V et al. Nucl. Phys. A, 2002, **703**: 222–239
13 REN Z Z, Toki H. Nucl. Phys. A, 2001, **689**: 691–706
14 König J, Ring P. Phys. Rev. Lett., 1993, **71**: 3079–3082
15 Arima A, Harvey M, Shimizu K. Phys. Lett. Sect. B, 1969, **30**: 517–522
16 Ginocchio J N. Phys. Rev. Lett., 1997, **78**: 436
17 Joseph N, Ginocchio. Phys. Rep., 2005, **414**(4–5): 165–261
18 MENG J, Sugawara-Tanabe K, Yamaji S et al. Phys. Rev. C, 1998, **58**(2): R628
19 LIANG H Z, SHEN S H, ZHAO P W et al. Phys. Rev. C, 2013, **87**: 014334
20 LV B N, ZHAO E G, ZHOU S G. Phys. Rev. C, 2013, **88**: 024323
21 GENG L S, Toki H, Sugimoto S, MENG J. Prog. Theor. Phys., 2003, **110**: 921
22 TIAN Y, MA Z Y, Ring P. Phys. Rev. C, 2009, **80**: 024313
23 MENG J, GUO J Y, LIU L et al. Front. Phys. China, 2006, **1**: 38–46
24 ZENG J Y, CHENG T S. Nucl. Phys. A, 1983, **405**: 1–28
25 ZENG J Y, LEI Y A, JIN T H et al. Phys Rev C, 1994, **50**: 746
26 LIU S X, ZENG J Y. Phys. Rev. C, 2002, **66**(6): 067301
27 LIU S X, ZENG J Y, ZHAO E G. Phys. Rev. C, 2002, **66**(2): 024320
28 WU X, ZHANG Z H, ZENG J Y et al. Phys. Rev. C, 2011, **83**(3): 034323
29 ZHANG Z H, HE X T, ZENG J Y et al. Phys. Rev. C, 2012, **85**(1): 014324
30 ZHANG Z H, MENG J, ZHAO E G et al. Phys. Rev. C, 2013, **87**(5): 054308
31 LIU L, ZHAO P W. Chin. Phys. C, 2012, **36**: 818–822
32 ZHANG Z H, ZHAO P W, MENG J et al. Phys. Rev. C, 2013, **87**(5): 054314
33 LONG W, MENG J, Van Giai N et al. Phys. Rev. C, 2004, **69**(3): 034319
34 WANG M, Audi G, Wapstra A H et al. Chin. Phys. C, 2012, **36**: 1603–2014
35 Ring P, Schuck P. The Nuclear Many-Body Problem. Springer, 2004